Available online at www.sciencedirect.com

ScienceDirect

Energy Procedia 114 (2017) 2182 – 2192

Energy Procedia

13th International Conference on Greenhouse Gas Control Technologies, GHGT-13, 14-18 November 2016, Lausanne, Switzerland

Carbon dioxide capture by pressure swing adsorption

Rafael M. Siqueira[a], Geovane R. Freitas[a], Hugo R. Peixoto[a], Jailton F. do Nascimento[b], Ana Paula S. Musse[b], Antonio E.B. Torres[a], Diana C.S. Azevedo[a], Moises Bastos-Neto[a,*]

[a]*Universidade Federal do Ceará, Departamento de Engenharia Química, 60455-760, Fortaleza - CE, Brazil*
[b]*PETROBRAS/CENPES, Av Horácio Macedo, 950 - Cidade Universitária - Ilha do Fundão, 21941-915, Rio de Janeiro – RJ, Brazil*

Abstract

The increasing worldwide demand for energy bound to a strong dependence of fossil fuels has considerably intensified the concentration of greenhouse gases in the atmosphere, reaching alarming levels. Among those gases, carbon dioxide is considered the main responsible for global warming due to its higher concentration. In order to mitigate the negative effects of global warming and to reduce emissions, many technologies have been developed in the last decades to separate and recover carbon dioxide (CO_2) at different capture scenarios. Adsorption processes rely on the use of highly porous solids such as activated carbons, which are either commercially. Pressure Swing Adsorption (PSA) is a cyclic adsorption process, which allows continuous separation of gas streams. PSA is performed by periodic changes of pressure aiming the optimization of contaminants removal and is considered viable for separation of CO_2 from flue gases containing about 5-15% v/v. To achieve a certain performance, a PSA process may consist of several steps, columns and cycle time. One of the most basic configurations comprises four steps: pressurization, feed, blowdown and purge. The performance of a PSA process is usually evaluated by the purity, recovery and productivity reached. This study presents experimental and simulated data obtained from a bench-scale PSA, with a maximum pressure of 6 bar for pressurization and feed steps and minimum of 1 bar for blowdown and purge steps. The unit was tested with a mixture containing 85% of N_2 and 15% of CO_2 (on a molar basis). Carbon dioxide and nitrogen breakthrough curves were obtained under typical conditions of post combustion capture. A mathematical-phenomenological model combining momentum, mass and heat balances and using the Linear Driving Force approach (LDF) for mass transport and Langmuir model for equilibrium was applied in this study to simulate the dynamic behavior of the process. The performance tests presented productivity of 15 mol h^{-1} kg-ads^{-1} and, according to the changes of step time, N_2 purity of 97.7%. The model predicted reasonably the breakthrough curves and temperature profiles, with more precision for the latter. The combination of the simulation tool with and experimental PSA unit is very valuable for a deeper understanding of the involved phenomena and helpful with the design of optimized and efficient CO_2 adsorption-based capture processes.

Peer-review under responsibility of the organizing committee of GHGT-13.

* Corresponding author. Tel.: +55-85-3366-9240; fax: +55-85-3366-9610.
E-mail address: moises@gpsa.ufc.br

Peer-review under responsibility of the organizing committee of GHGT-13.
doi:10.1016/j.egypro.2017.03.1355

Keywords: adsorption; CCS; PSA

1. Introduction

The increasing worldwide demand for energy bound to a strong dependence of fossil fuels has considerably intensified the concentration of greenhouse gases in the atmosphere, reaching alarming levels. According to IPCC report [1], the largest sources of greenhouse gases were the sectors of energy production, agriculture, forestry and land-use. Looking at the total source of greenhouse gases at present CO_2 contributes 76 %; CH_4 about 16 %, N_2O about 6 % and the combined F-gases about 2 % [1]. Among those gases, carbon dioxide is considered the main responsible for global warming due to the relative high concentration in atmosphere. In order to mitigate the negative effects of global warming and to reduce emissions, several studies [2–6] present many technologies that have been developed in the last decades to separate and recover carbon dioxide (CO_2) at different capture scenarios.

Gas separation on a large scale is an important task of many industrial processes. Absorption, cryogenic distillation, membrane separation, adsorption are some examples of processes developed for such a purpose [7]. From these techniques, adsorption stands out as a promising operation due to its relative low cost and energy efficiency [8, 9]. Adsorption processes rely on the use of highly porous solids such as activated carbons, which are either commercially available or under development through research on material science and engineering. Carbon Capture and Storage is a viable process that can be implemented in an energy infrastructure. CCS consists in CO_2 sequestration from an exhaust gas and stored for a long time [10, 11]. In respect to capture CO_2 by adsorption process, the most used technology in industrial scale is Pressure Swing Adsorption (PSA). It is a cyclic adsorption process, which allows continuous separation of gas streams. PSA is performed by periodic changes of pressure aiming the optimization of contaminants removal and is considered viable for separation of CO_2 from flue gases containing about 5-15% v/v [12, 13].

The choice of the adsorbent is critical to the effective operation of a PSA unit. The properties of the adsorbents are one of the most important aspects of the unit performance for a given cycle configuration [14]. Most adsorbents have surfaces which interact most strongly with CO_2 than N_2. These materials are commonly referred to equilibrium adsorbent, e.g., activated carbon, zeolites and metal-organic frameworks (MOFs). Other adsorbents show little difference from the adsorption capacity in balance of the blend components, but the rates of diffusion in the micropores are distinct, leading to a kinetic separation nature. Some studies have shown that "kinetic adsorbents" can result in better performance in a PSA unit compared to "adsorbents the equilibrium base" because of the strong nonlinearity ("irreversibility") of the isotherms of the latter [15]. The design of a PSA process is a very complex task. To achieve a certain performance, a PSA process may consist of several steps, columns, different cycle time, choice of the adsorbents, bed length and composition of the gas mixture at the column inlet. One of the most basic configurations procedures comprises four steps: pressurization, feed, blowdown and purge. The performance of a PSA process is usually evaluated by the purity, recovery and productivity reached. As it is known, for valuation of an experimental PSA process it is required large amount of gases and time of experiment which becomes it infeasible. However, for a developed mathematical model that agree with the experimental data it can have a great economic viability. To be used with confidence, this model must be tested several times with different configurations and one way to be done it is by using a laboratory scale PSA unit [16].

This work aims to evaluate the performance of a PSA unit to separate N_2/CO_2 at a composition similar to those of flue gases (85/15%) using the most basic cyclic process of a PSA process (Skarstrom cycle) and a commercial activated carbon as adsorbent. Additionally, a mathematical model was developed to the process dynamics in order to better understand the involved phenomena and help designing more efficient process configurations.

2. Materials and methods

2.1. Assessment of adsorption equilibrium

Single component and binary equilibrium data were obtained by using a Rubotherm (Bochum, Germany) magnetic suspension balance. Adsorption measurements were performed at 25, 50 and 75 °C at pressures ranging from vacuum (10^{-3} bar) up to 20 bar. The adsorbent regeneration was carried out at 150 °C under vacuum for 6 hours with heating rate of 1 °C min^{-1}. CO_2 (99.5%) and N_2 (99.999%) were supplied by White Martins Praxair Inc. (Brazil). Equilibrium was assumed to be reached when the mass variation was less than 10^{-4} g for at least 30 min. Data handling and determination of adsorbed amounts were performed according to the literature [17–19].

2.2. Isotherm models

The Langmuir isotherm model (Eq. 1) was fitted to the experimental single component adsorption data. It describes the formation of a monolayer assuming surface homogeneity and energetically equivalent adsorption sites with no interactions between adjacent sites [20-21].

$$q = \frac{q_m b P}{(1 + bP)} \tag{1}$$

where q is the adsorbed concentration (mmol g^{-1}) in equilibrium, while q_m (mmol g^{-1}) is the maximum adsorbed concentration or saturation capacity; b is related to the adsorbate-adsorbent affinity (bar^{-1}) and P the pressure (bar).

Parameter b is a function of temperature represented by Eq. 2.

$$b = b_0 e^{E_a * RT} \tag{2}$$

where the constants b_0 and E_a represent the pre-exponential factor and the energy of adsorption, respectively [22].

The extended Langmuir model (EL) (Eq. 3) was used to describe the adsorption of binary mixtures. This model uses the parameters obtained from the fittings for the isotherms of each component (i).

$$q_i = \frac{q_{m,i} b_i P_i}{(1 + \sum b_j P_j)} \tag{3}$$

2.3. Column dynamics and PSA cycles

A fixed bed unit was used to obtain breakthrough curves of pure components and mixtures (CO_2/N_2) diluted in helium (purity of 99.999%), which is assumed not to adsorb, at three different pressures (6, 12 and 20 bar) to provide data for the validation of the PSA mathematical model. For the (pseudo) single component breakthrough curves, CO_2 and N_2 were diluted in 90% of He. The composition for the runs with $He/CO_2/N_2$ was 24/16/60%, which gives a relationship of approximately 21:79 for CO_2:N_2, all in molar basis. The column was packed with an activated carbon sample with properties shown in Table 1. The total pressure inside the column was kept constant with the aid of a back-pressure controller (BPC) at bed outlet. The feed flow rate, controlled by mass flow controllers (MFC), was set to 5.4 L min^{-1} for the He/CO_2 and He/N_2 experiments and 6.8 L min^{-1} for the mixture CO_2/N_2/He. All volumetric flow rates reported in the present work are at standard condition of 1 atm and 273.15 K.

Table 1. Column and adsorbent properties

Column	
Fixed bed length	0.54 m
Inner diameter	0.028 m
Wall thickness	2.8×10^{-3} m
Wall density	7400 kg m^{-3}
Specific heat capacity wall	470 J kg^{-1} K^{-1}
Adsorbent	
Mass	0.136 kg
Specific pore volume	4.6×10^{-4} m^3 kg^{-1}
Specific solid volume	4.2×10^{-4} m^3 kg^{-1}
Particle diameter	3×10^{-4} m

The configuration used in the pilot-scale PSA unit for the experiments is shown in Fig. 1. Four elementary steps of a Skarstrom-type PSA cycle were used to perform the CO_2 separation process at a constant temperature of 298.15 K, with upper adsorption pressure of 6 bar and lower desorption pressure of 1 bar.

The PSA cycle started with a co-current pressurization step at the top of the bed, fed with the mixture CO_2+N_2 in a flow rate of 4.2 L min^{-1} and composition of 85% N_2 and 15% CO_2. In the second step, adsorption, the heavy component, CO_2 in the case, is removed from the mixture, with the same flow rate and composition at a constant pressure of 6 bar and temperature (298.15 K). Blowdown is the third step; a rapid counter-current depressurization until the bed pressure reaches the lowest pressure of the cycle (1 bar). A part of CO_2 is removed in this step. Finally, the cycle ends in the purge step where a flow rate of 0.15 L min^{-1} of pure N_2 flows counter-current through the fixed bed at a constant pressure of 1 bar. This step has the goal of remove a part of CO_2 adsorbed. A total number of 33 cycles was investigated.

The time of pressurization step (PR) was set according to the total flow rate; this step ended when the bed reached a pressure tolerance of 0.1 bar from the operational maximum pressure (6 bar). The adsorption step (AD) was set to last 70 seconds. Blowdown (BD) and purge (PG) steps must have the same time as pressurization and adsorption, respectively, in order to synchronize both columns. Before the experimental procedure, the adsorbent bed was pretreated by applying vacuum (2.1×10^{-3} kPa) and heated to around 423.15 K for six hours. Then, the columns were cooled down with the aid of a thermostatic bath until the experimental temperature (298.15 K) was reached. The whole procedure was monitored and operated through an interface created in LabView software (National Instruments Corp.), including control of valves, MFCs and BPC. The gas mixture composition was measured using a Gas Cromatograph Series 580 (Gow-Mac Instruments Co., USA).

A mathematical model was developed to better understand and predict the dynamics of PSA separation processes. Material, energy and momentum balances were applied to describe system. The momentum balance is given by the Ergun equation [23]. The energy balance considers fast thermal equilibrium between the solid (adsorbent) and fluid phase [24]. Further details regarding the model equation are available elsewhere [11, 24–27].

The following assumptions were made in this work: i) plug flow with axial mass dispersion; ii) mass transfer into the particle described according to the Linear Driving Force approach; iii) micropore diffusion controls the mass transfer resistance; iv) thermal equilibrium between the solid and fluid phase; v) no mass, heat or velocity gradients in the radial direction; vi) constant heat transfer coefficients; vii) mass in the column 1 is the same of the column 2; viii) ideal gas behavior.

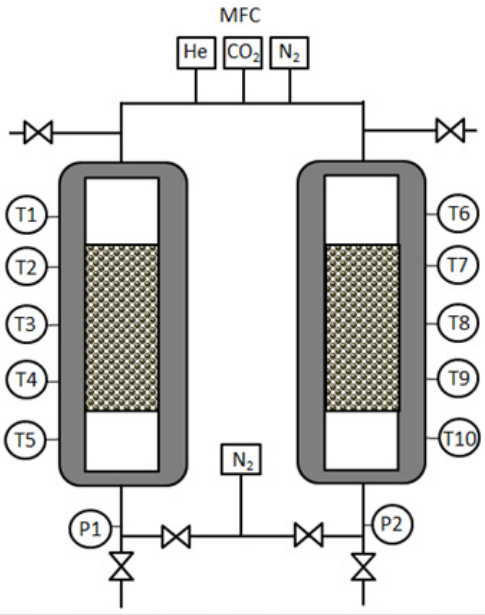

BED 1	Pressurization	Adsorption	Blowdown	Purge
BED 2	Blowdown	Purge	Purge	Adsorption

Fig. 1 - Schematic illustration of the two-bed PSA unit and the steps for each bed

Based on the pore structure of the activated carbon sample used in this work, it was assumed that the external mass transfer and macropores diffusion resistances are insignificant when compared to the micropore diffusion resistance. Hence, the mass transfer coefficient (k_{LDF}) was based only on micropore diffusivity and determined by fitting the model to experimental breakthrough curves. The average rate of concentration change in the adsorbed phase is expressed by Eq. 4.

$$\frac{\partial \bar{q}_i}{\partial t} = k_{LDF}\left(q_i^* - \bar{q}_i\right) \tag{4}$$

where $\bar{q}_i$ is the average adsorbed amount of component *i* and q_i^* is the actual adsorbed amount in equilibrium.

The axial dispersion coefficient was calculated according to the correlation of Wakao and Funazkri [29].

$$\varepsilon_b \frac{D_{ax}}{D_m} = \varepsilon_0 + 0.5\,\mathrm{Re}\,Sc \tag{5}$$

where the parameter ε_0 corresponding to the stagnant contribution to axial dispersion, which, in the present case, given the low Reynolds number, was set to 0.23. For higher Reynolds regimes, the value of that parameter is commonly set to 20 [24, 25, 29, 30]. The molecular diffusivity (D_m) was calculated using the Chapman-Enskog equation [23]. Other parameters are calculated according to correlations presented in Table 2.

In Table 2, λ_L and κ_g represent the axial heat dispersion coefficient and the thermal conductivity in the gas phase, respectively, in J s^{-1} m^{-1} K^{-1}; h_w is the wall heat transfer coefficient; d_{int} and d_{ext} are the internal and external column diameter, respectively; d_p is the particle diameter; k_w is the wall thermal conductivity; μ_g is the viscosity of the gas mixture and u is the superficial velocity of the gas.

Table. 2. Parameters used in all simulation processes

Parameter	Correlation
Axial heat dispersion	$\frac{\lambda_L}{k_g} = 7 + 0.5\,Sc\,\mathrm{Re}$
Global heat transfer	$U = \frac{1}{(1/h_w) + (d_{\mathrm{int}}/k_w)\ln(d_{ext}/d_{\mathrm{int}}) + (d_{\mathrm{int}}/d_{ext})(1/h_{ext})}$
Schmidt Number	$Sc = \frac{\mu_g}{\rho_g D_m}$
Reynolds Number	$\mathrm{Re} = \frac{\rho_g u d_p}{\mu_g}$

The performance of a PSA process is commonly evaluated through the product purity, product recovery and productivity. Those three parameters can be calculated according to Eqs. 6-8 [31–33]. The system was equipped with a gas analyzer (GC) equipped with a thermal conductivity detector at the exit of the column. The samples of the gas mixture leaving the column were collected and stored automatically into the analyzer, for posterior analysis.

$$N_2\ Purity = \frac{\sum_{AD}\left(\int_0^{t_{AD}} F_{N_2,out}\,dt\right)}{\sum_{AD}\left(\int_0^{t_{AD}} F_{N_2,out}\,dt + \int_0^{t_{AD}} F_{CO_2,out}\,dt\right)} \tag{6}$$

$$N_2\ \mathrm{Recovery} = \frac{\sum_{AD}\left(\int_0^{t_{AD}} F_{N_2,out}\,dt\right) - \sum_{PG}\left(\int_0^{t_{PG}} F_{N_2,in}\,dt\right)}{\sum_{AD}\left(\int_0^{t_{AD}} F_{N_2,in}\,dt\right) + \sum_{PR}\left(\int_0^{t_{PR}} F_{N_2,in}\,dt\right)} \tag{7}$$

$$N_2\ \mathrm{Prod.} = \frac{\sum_{AD}\left(\int_0^{t_{AD}} F_{N_2,out}\,dt\right) - \sum_{PG}\left(\int_0^{t_{PG}} F_{N_2,out}\,dt\right) - \sum_{PR}\left(\int_0^{t_{PR}} F_{N_2,\mathrm{in}}\,dt\right)}{mass\ of\ dry\ adsorbent \times t_{cycle}} \tag{8}$$

where AD, BD, PR, PG are the steps of the PSA process as previously described. In this case, the productivity of nitrogen is determined in mol kg^{-1} h^{-1}.

3. Results

3.1. Adsorption isotherms

Adsorption equilibrium isotherm data for pure component CO_2 and N_2 at 298, 323 and 348 K are shown in Fig. 2 and the isotherm for the mixture CO_2 + N_2 (15/85 %) at 298 K is presented in Fig. 3. The parameters of the Langmuir model fitted to the experiments are exhibited in Table 3.

As one can observe, the Extended Langmuir model was able to satisfactorily predict the behavior of the mixture adsorbing by using the parameters obtained from the fitting for each component. The activated carbon sample presented a higher capacity for carbon dioxide in comparison to nitrogen, as expected, since CO_2 critical temperature (304.45 K) is significantly higher than that of N_2 (126.19 K), which makes CO_2 behave more like a condensable vapor and not as a supercritical gas as occurs with N_2.

The isosteric heat of adsorption is a necessary input parameter for the energy balance, evaluated from the isotherms by applying the Clausius-Clapeyron equation [22]. The obtained heats of adsorption for CO_2 and N_2 as functions of the amount adsorbed are shown in Figure 4. The variation of the heats of adsorption were neglected and an average value of 26 kJ mol^{-1} was used for CO_2 and 15 kJ mol^{-1} for N_2.

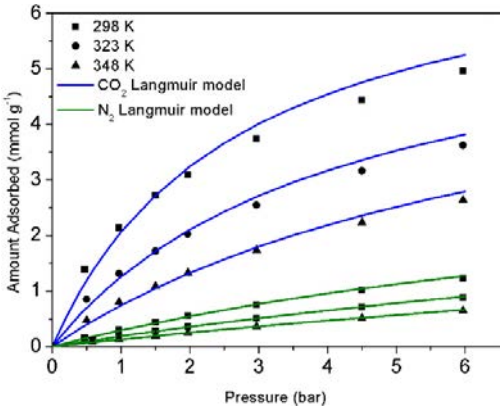

Fig. 2. Single-component isotherms at 298, 323, 348 K for CO_2 and N_2. Symbols are experimental data and lines the Langmuir model fit.

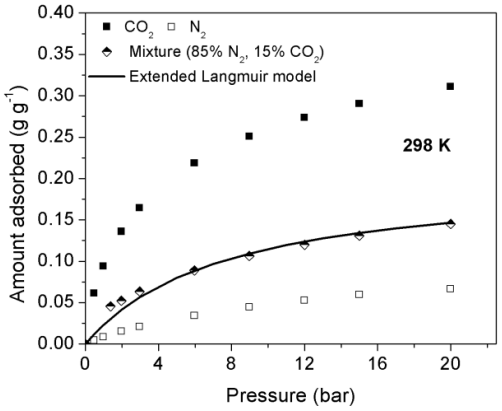

Fig. 3. Adsorption equilibrium isotherms for CO_2, N_2 and mixture. Symbols are experimental data and continuous line the model.

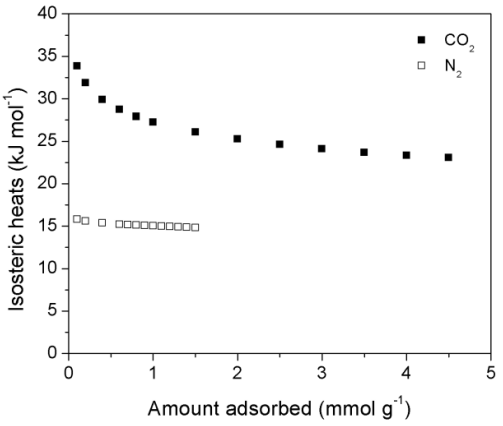

Fig. 4. Isosteric heats of adsorption for CO_2 and N_2 as a function of the amount adsorbed.

Table 3. Langmuir model parameters used in simulation process

Langmuir model parameter	CO_2	N_2
q_m (kmol kg^{-1})	6.123	2.876
b (bar^{-1})	0.5550	0.1134
E_a (J mol^{-1})	-16180	-15072

3.2. Column dynamics and PSA runs

Experimental and simulated breakthrough curves with 10% of molar concentration at 6, 12 and 20 bar are presented in Figs. 5a and 5b, for CO_2 and N_2, respectively. The simulated curves are in good agreement with the experimental results at all different all studied conditions for both gases. The breakthrough curves for the mixture CO_2/N_2 diluted in helium at 6 bar are exhibited in Fig. 5c. In accordance to the equilibrium data (isotherms) one can notice that N_2 leaves the column earlier than CO_2, indicating higher retention capacity for the latter.

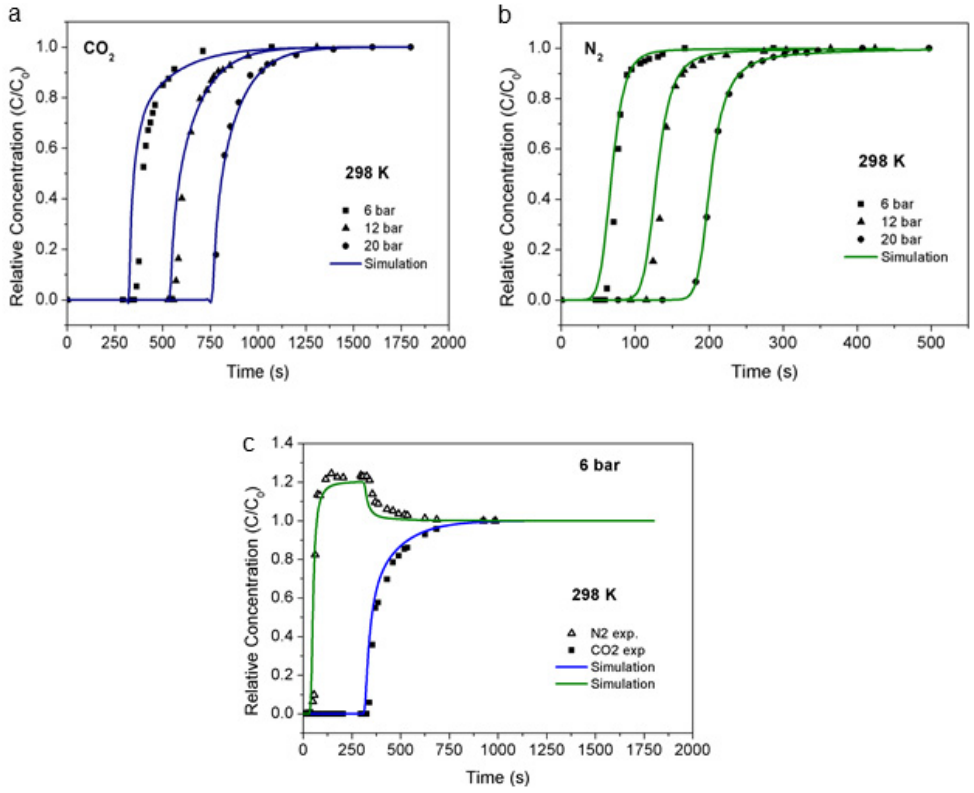

Fig. 5 - Breakthrough curves for (a) CO_2, (b) N_2 and (c) CO_2/N_2 in He. Symbols are experimental data and continuous lines simulations.

After the fixed-bed model validation and observation of the time necessary for CO_2 to break through the column, the next step was to run the PSA cycles as described in the previous section. As mentioned before, nitrogen and carbon dioxide were dosed to the PSA unit in a composition ratio similar to typical values for flue gases (i.e. 85% of N_2 and 15% of CO_2). With a pressurization time of 58 seconds in average, the PSA process was performed in 33 cycles, reaching the cyclic stationary stage (CSS) around the 25th.

The pressure profile inside the adsorption bed of the first two cycles and the simulated pressure data are displayed in Fig. 6, showing good agreement between each other. Gas phase samples were collected in the end of the adsorption step at different moments along the PSA cycles, so that the composition could be analyzed. According to the obtained results, the achieved N_2 purity and productivity were then evaluated as shown in Fig. 7.

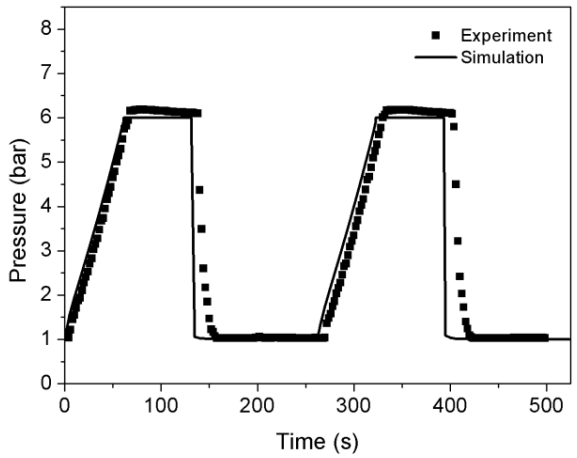

Fig. 6. History of the pressure of the two first cycles at the column outlet during the CO_2 separation process by PSA.

Again, comparison between experimental and simulation data assures the reliability of the model. According to the results for the tested process configuration and step program, a purity of about 98% and productivity of 15 mol h^{-1} kg-ads^{-1} are reached at cyclic steady state.

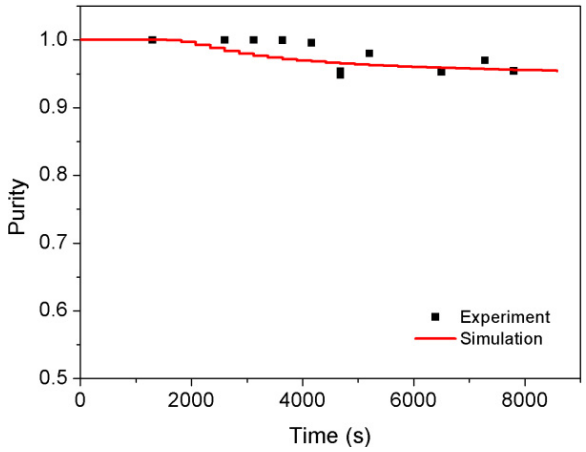

Fig. 7. History of the N_2 purity during the CO_2 separation process by PSA. Symbols for experimental data and continuous line for simulation.

4. Conclusions

A mathematical model was developed to describe the dynamic behavior of a cyclic CO_2 separation by adsorption in porous media. The model was tested and validated with experimental data obtained in a pilot-scale dual-bed PSA unit. The model was fed with equilibrium, kinetics and heat parameters in order to solve the balances.

The extended Langmuir model has satisfactorily predicted adsorption data for the mixture CO_2/N_2, by using the parameters obtained by the fitting for each gas. The commercial activated carbon sample showed higher adsorption capacity for CO_2 with respect to N_2, which was expected due to the physical properties of the first.

The use of correlations and approaches presented in the literature to determine transport coefficients and conductivities lead to satisfactory results since simulations of breakthrough curves and PSA cycles showed very good agreement with experimental data.

According to the proposed process configuration, a purity of N_2 of about 98% and productivity of 15 mol h^{-1} kg-ads^{-1} have been achieved at the 25^{th} , when the system reaches the cyclic stationary stage.

The objective of this work has been reached, given the accuracy of the predictions obtained with the model. The combination of the simulation tool with and experimental PSA unit is very valuable for a deeper understanding of the involved phenomena and helpful with the design of optimized and efficient CO_2 adsorption-based capture processes.

The next step is to optimize the process configuration so that higher purities and productivities could be attained using a given adsorbent material with well-known properties.

Acknowledgements

The authors acknowledge financial support from the Brazilian National Agency of Petroleum, Natural Gas and Biofuels (*Agência Nacional de Petróleo, Gás Natural e Biocombustíveis* – ANP, Brazil) and PETROBRAS through the Clause of Investments in Research, Development and Innovation (*Cláusula de Investimentos em Pesquisa, Desenvolvimento e Inovação*) in the contracts for Exploration, Development and Production of Petroleum and Natural Gas.

References

[1] Victor DG, Zhou D, Ahmed EHM, Dadhich PK, Olivier JGJ, Rogner H-H, Sheikho K, Yamaguchi M.: Introductory Chapter. In: Climate Change 2014: Mitigation of climate change. Contribution of working group III to the fifth assessment report of the intergovernamental panel on climate change. [Edenhofer O, Pichs-Madruga R, Sokona Y, Farahani E, Kadner S, Seyboth K, Adler A, Baum I, Brunner S, Eickemeier P, Kriemann B, Savolainen J, Schlömer S, von Stechow C, Zwickel T and Minx JC (eds)]. Cambridge University Press, New York; 2014.

[2] Webley PA. Adsorption technology for CO_2 separation and capture: A perspective. Adsorption 2014; 20, no. 2–3, pp. 225–231.

[3] Sreenivasulu B, Gayatri DV, Sreedhar I, Raghavan KV. A journey into the process and engineering aspects of carbon capture technologies. Renew. Sustain. Energy Rev 2015; 41, 1324–1350.

[4] Ben-Mansour R, Habib MA, Bamidele OE, Basha M, Qasem NAA, Peedikakkal A, Laoui T, Ali M. Carbon capture by physical adsorption: Materials, experimental investigations and numerical modeling and simulations - A review. Appl. Energy 2016; 161, 225–255.

[5] Berghout N, van den Broek M, Faaij A. Techno-economic performance and challenges of applying CO_2 capture in the industry: A case study of five industrial plants. Int. J. Greenh. Gas Control 2013;17, 259–279.

[6] Rufford TE, Smart S, Watson GCY, Graham BF, Boxall J, Diniz da Costa JC, May EF. The removal of CO_2 and N_2 from natural gas: A review of conventional and emerging process technologies. J. Pet. Sci. Eng 2012; 94:95, 123–154.

[7] Wiersum AD, Chang JS, Serre C, Llewellyn PL. An adsorbent performance indicator as a first step evaluation of novel sorbents for gas separations: Application to metal-organic frameworks. Langmuir 2013; 29: 10, 3301–3309.

[8] Mondal MK, Balsora HK, Varshney P. Progress and trends in CO_2 capture/separation technologies: A review. Energy 2012; 46: 1, 431–441.

[9] Leung DYC, Caramanna G, Maroto-Valer MM. An overview of current status of carbon dioxide capture and storage technologies. Renew. Sustain. Energy Rev. 2014; 39, 426–443

[10] Hedin N, Andersson L, Bergström L, Yan J. Adsorbents for the post-combustion capture of CO_2 using rapid temperature swing or vacuum swing adsorption. Appl. Energy 2013; 104, 418–433.

[11] Nikolaidis GN, Kikkinides ES, Georgiadis MC. Model-Based Approach for the Evaluation of Materials and Processes for Post-Combustion Carbon Dioxide Capture from Flue Gas by PSA / VSA Processes. Ind. Eng. Chem. Res. 2016; 55, 635-646.

[12] Ruthven DM. Principles of Adsorption and Adsorption Processes. New York: John Wiley & Sons, 1984.
[13] Yang RT, Gas separation by adsorption process, Butterwort. Boston, 1997.
[14] Maring BJ and Webley PA. A new simplified pressure/vacuum swing adsorption model for rapid adsorbent screening for CO_2 capture applications. Int. J. Greenh. Gas Control 2013; 15, 16–31.
[15] Grande CA and Rodrigues AE. Biogas to fuel by vacuum pressure swing adsorption I. Behavior of equilibrium and kinetic-based adsorbents. Ind. Eng. Chem. Res.2007; 46: 13, 4595–4605.
[16] Marx D, Joss L, Hefti M, Gazzani M, Mazzotti M. CO_2 Capture from a Binary CO_2 / N_2 and a Ternary CO_2 / N_2 / H_2 Mixture by PSA : Experiments and Prediction. Ind. Eng. Chem. Res. 2015; 54, 6035-6045.
[17] Dreisbach F and Löch HW. Highest Pressure Adsorption Equilibria Data : Measurement with Magnetic Suspension Balance and Analysis with a New Adsorbent / Adsorbate-Volume. Adsorption 2002; 8, 95–109.
[18] Bastos-Neto M, Canabrava DV, Torres AEB, Rodriguez-Castellón E, Jiménez-López A, Azevedo DCS, Cavalcante Jr CL. Effects of textural and surface characteristics of microporous activated carbons on the methane adsorption capacity at high pressures. Appl. Surf. Sci. 2007; 253: 13 SPEC. ISS., 5721–5725.
[19] Vilarrasa-García E, Cecilia JA, Bastos-Neto M, Cavalcante Jr CL, Azevedo DCS, Rodriguez-Castellón E. CO_2/CH_4 adsorption separation process using pore expanded mesoporous silicas functionalizated by APTES grafting. Adsorption 2015; 21, 565–575.
[20] Langmuir I. The adsorption of gases on plane surfaces of glass, mica and platinum. J. Am. Chem. Soc. 1918; 40, 1361-1402.
[21] Do DD and Wang K. A New Model for the Description of Adsorption Kinetics in Heterogeneous Activated Carbon. Carbon N. Y. 1998; 36, 10, 1539–1554.
[22] Rouquerol F, Rouquerol J, Sing KSW, Llewellyn P, Maurin G. Adsorption by powders & porous solids – Principles methodology and applications, 2nd ed. London, 2014.
[23] Bird RB, Stewart WE, Lightfoot E, Transport Phenomena, 2nd ed. New York, 2006.
[24] Bastos-Neto M, Moeller A, Staudt R, Böhm J, Gläser R. Dynamic bed measurements of CO adsorption on microporous adsorbents at high pressures for hydrogen purification processes. Sep. Purif. Technol. 2011; 77: 2, 251–260.
[25] Ferreira AFP, Ribeiro AM, Kulaç S, Rodrigues AE. Methane purification by adsorptive processes on MIL-53(Al). Chem. Eng. Sci. 2015; 124, 79–95.
[26] Ribeiro AM, Grande CA, Lopes FVS, Loureiro JM, Rodrigues AE. A parametric study of layered bed PSA for hydrogen purification. Chem. Eng. Sci. 2008; 63: 21, 5258–5273.
[27] Santos MS, Grande CA, Rodrigues AE. New cycle configuration to enhance performance of kinetic PSA processes. Chem. Eng. Sci. 2011; 66: 8,1590–1599.
[28] Luberti M, Kim YH, Lee CH, Ferrari MC, Ahn H. New momentum and energy balance equations considering kinetic energy effect for mathematical modelling of a fixed bed adsorption column. Adsorption 2015; 21: 5, 353–363.
[29] Wakao N and Funazkri T. Effect of fluid dispersion coefficients on particle-to-fluid mass transfer coefficients in packed beds. Chem. Eng. Sci. 1978; 33, 1375–1384.
[30] Dantas TLP, Luna FMT, Silva IJ, Torres AEB, Azevedo DCS, Rodrigues AE, Moreira RFPM. Carbon dioxide-nitrogen separation through pressure swing adsorption. Chem. Eng. J. 2011; 172:2–3, 698–704.
[31] Cavenati S, Grande CA, Rodrigues AE. Separation of CH_4/CO_2/N_2 mixtures by layered pressure swing adsorption for upgrade of natural gas. Chem. Eng. J. 2006; 118: 3,3893–3906.
[32] Kacem M, Pellerano M, Delebarre A. Pressure swing adsorption for CO_2 / N_2 and CO_2 / CH_4 separation : Comparison between activated carbons and zeolites performances. Fuel Process. Technol. 2015; 138, 271–283.
[33] Riboldi L, Bolland O, Ngoy JM, Wagner N. Full-plant analysis of a PSA CO_2 capture unit integrated in coalfired power plants: post- and pre-combustion scenarios. Energy Procedia 2014; 63: 1876, 2289–2304.
[34] Yan H, Fu Q, Zhou Y, Li D, Zhang D. International Journal of Greenhouse Gas Control CO_2 capture from dry flue gas by pressure vacuum swing adsorption : A systematic simulation and optimization. Int. J. Greenh. Gas Control 2016; 51, 1–10.